Chapter 5

RESULTS AND DISCUSSION

1.1 Introduction

In this chapter discuss the result of proposed Rainfall prognostic artificial model framework and discharge prediction from Hydrological models (HEC-HMS and SWAT) and Data driven models or soft computing technique (Random Forest and M5P Models). It also discusses the model errors from simulation result, infiltration rate with runoff level and steep slopes of the velocity field using the Posterior fire-breathing network, Prophetic Multilayer Network, and well-ordered selective genetic algorithm. Compare of the Results of HEC-HMS vs Random Forest (RF) and SWAT vs M5P models is also discussed.

1.2 Simulation results

Simulation Analysis of the proposed Rainfall prognostic artificial model framework is presented in the section. Simulated results show the model errors, infiltration rate with runoff level, and steep slopes of the velocity field using the Posterior fire-breathing network, Prophetic Multilayer Network, and well-ordered selective genetic algorithm. The several parameters are taken to estimate the performance of the proposed framework such as precision probabilistic discharge with and without error, infiltration rate of soil, velocity of water in different bend areas. Those parameters are considered to estimate accurate day by day prediction as well as month vise prediction. The infiltration rate affects the run off prediction so that the soil infiltration rate and discharge is estimated.

Figure 5.1 states the Rainfall flow region between the years 1900 to 2020. The proposed rainfall prognostic model-based artificial framework predicts the rainfall in the year range from 1900-2020.

From the year 1900 to 1920, the average predicted rainfall level gradually increased to 1500 mm from 1025 mm. This is the highest rainfall level marked to date in the dataset. Then the rainfall value is 1400 mm predicted and gets constant for several years like 1935, 1960, and 1990. The marked average rainfall value for a couple of years is less compared to the early stage. The predicted rainfall value in the prognostic network of the proposed model is approximately 915 to 930 mm.

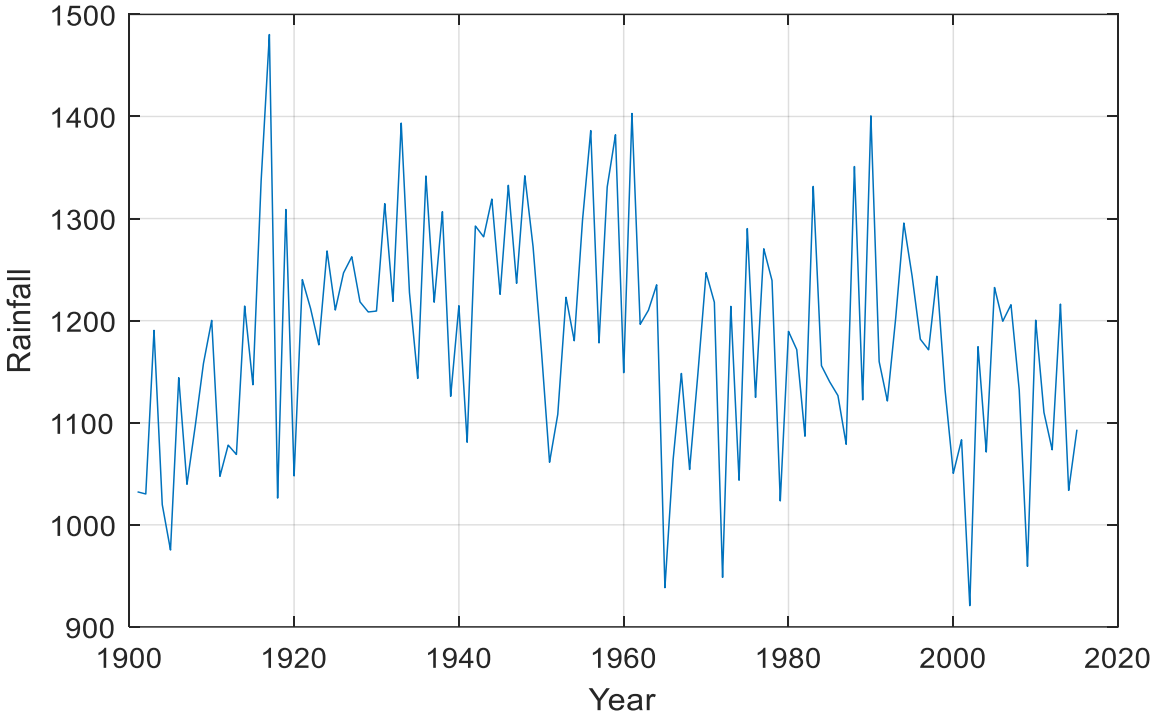

Figure 1.1: Rainfall Region

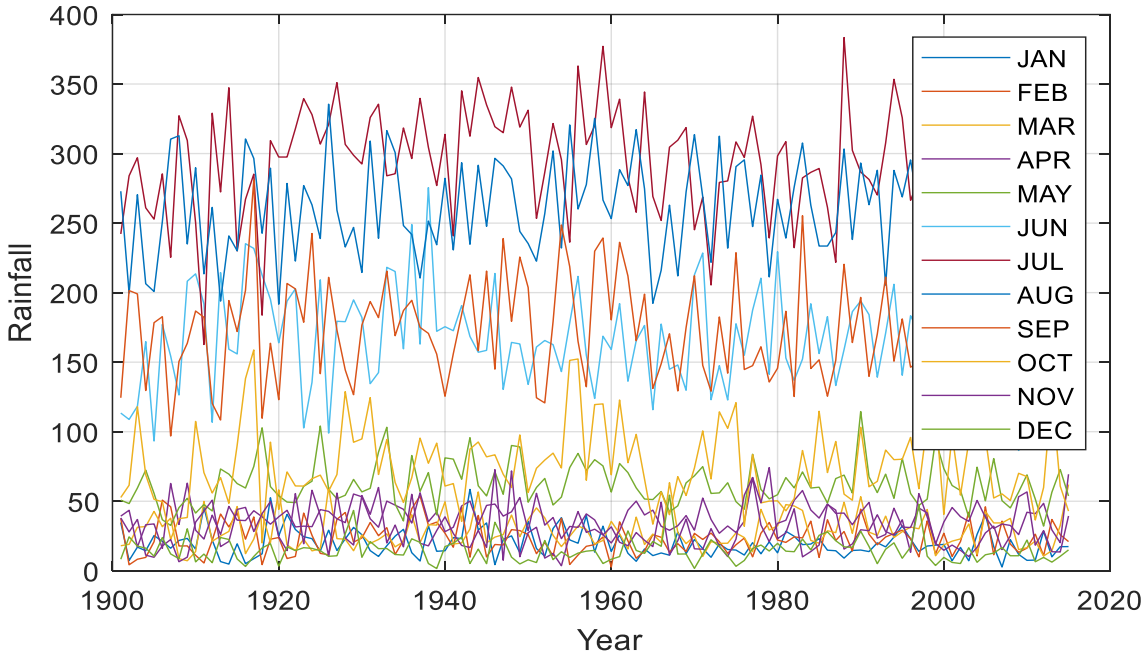

Figure 1.2: Month-wise rainfall in India

Figure 5.2 states the rainfall-runoff in month wise (i.e., January, February, March, April, May, June, July, August, September, October, November, and December). Each month's rainfall level in India between the years 1900-2020 is represented in figure 5.2. The predicted rainfall and measured rainfall is given in table 5.1, here the input is year and the output is rainfall measured in mm.

Table 5.1 provides a comprehensive overview of both the observed (measured) and forecasted (predicted) rainfall data. This table offers a valuable comparison spanning the time frame from 1990 to 2020, allowing us to assess the accuracy of the predictive models in capturing rainfall trends over this substantial period. Within this table, it has been observed that the values of predicted rainfall closely align with the measured rainfall data for the years spanning 1990 to 2020. This alignment suggests that the predictive models employed in this study effectively capture and replicate the historical rainfall patterns over this extended timeframe.

For instance, an examination was conducted in the year 1990, where it was observed that the predicted rainfall amount is 375 mm, while the measured rainfall for the same year is 376.3 mm. This demonstrates a high level of accuracy and reliability in the predictive models, as the predicted value is in very close proximity to the actual observed value.

In summary, Table 5.1 serves as a crucial reference point for assessing the performance of the predictive models, indicating their ability to replicate historical rainfall data effectively. It highlights the remarkable consistency between predicted and measured rainfall values, which is particularly evident in the example of the year 1990, further emphasizing the reliability and utility of the predictive models within this study.

Table 1.1: predicted rainfall vs measured rainfall

year	Predicted rain fall(mm)	Measured rain fall (mm)
1990	375	376.3
2002	950.2	936.4
2005	215	212.2
2009	975.9	974.9
2019	1285	1,284
2020	1170.5	1177

Figure 5.3 compares the real posterior at a particular time step with the Gamma approximation achieved through iteration. The iterative process commences from the prior for that time step, progressively refining the approximation to closely match the actual posterior. This results in

a robust posterior approximation facilitated by the precision of the prior density converging towards the posterior approximation.

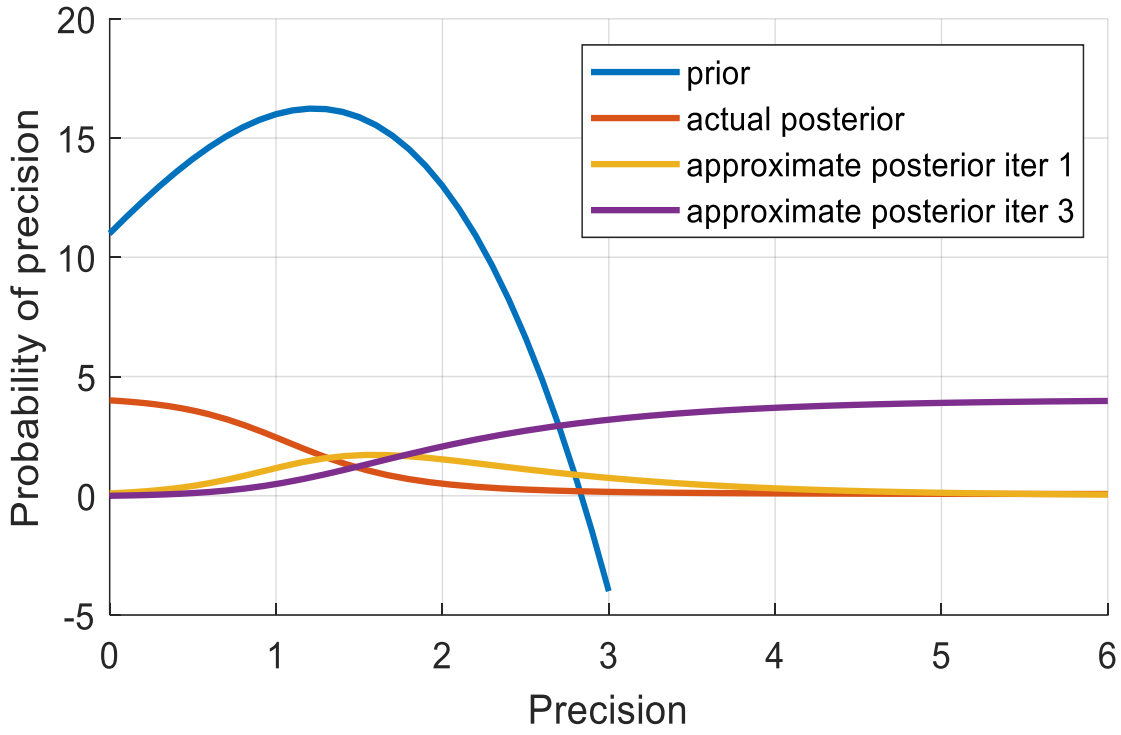

Figure 1.3: Approximating the actual posterior of τ a Gamma density by iterating, starting from the prior

Also, the gamma density from the prior network reaches maximum of 15% probability precision. Due to the presence of gamma approximation, the network is tuned for new values.

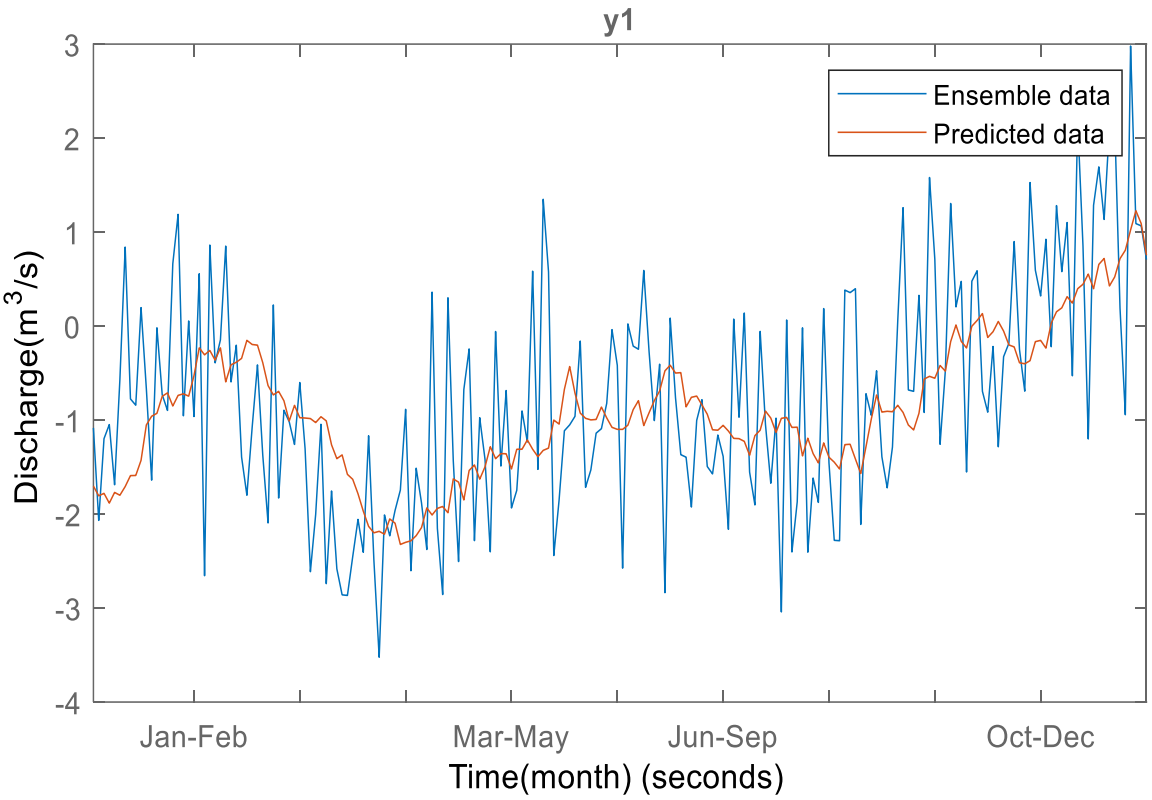

Figure 1.4: One-day-ahead probabilistic discharge prediction

In Figure 5.4, observe the dynamic evolution of the estimated posterior. The posterior fire-breathing network is recursively updated with each new measurement. Over time, the posterior fluctuates in response to the disparity between predicted and observed discharge. The value rises during periods of small error and decreases during periods of large error, reflecting the automatic ensemble Kalman Filter deflation to ensure accurate rainfall discharge without model errors in predictive and observation distributions.

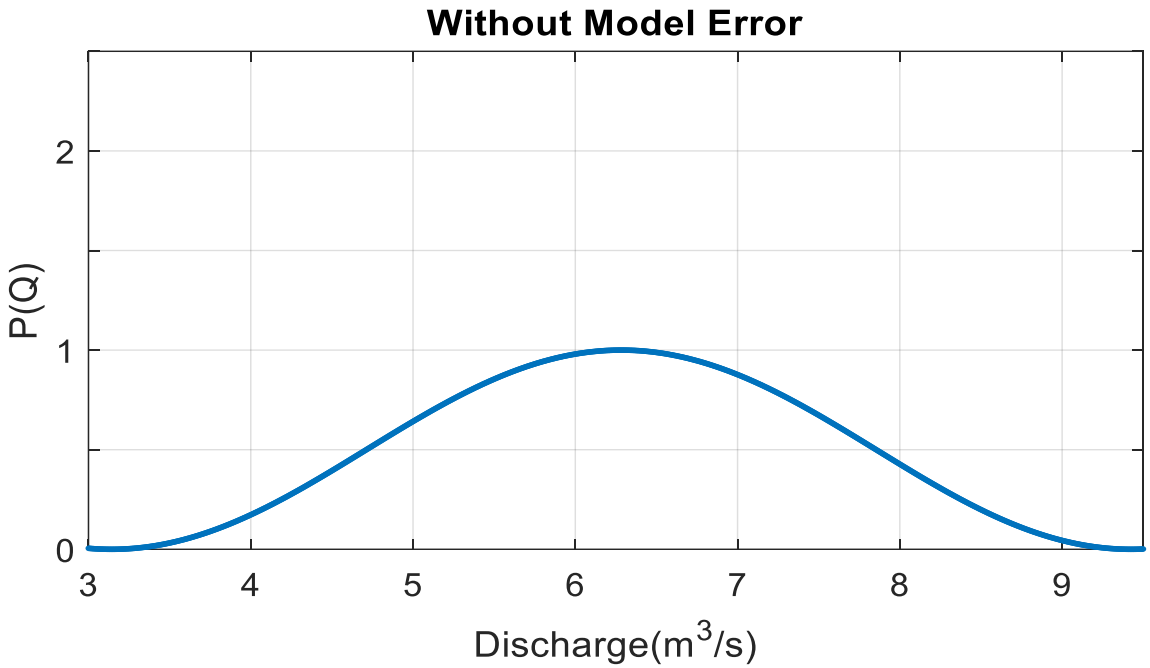

Figure 1.5: Without Model Error

Figure 5.5 shows without model error the predictive distribution is already quite good, and the predictive distribution with model error becomes too wide when compared to the likelihood. The results in a shift of the posterior τ , find smaller model noise. In the model, without error, the probability is one.

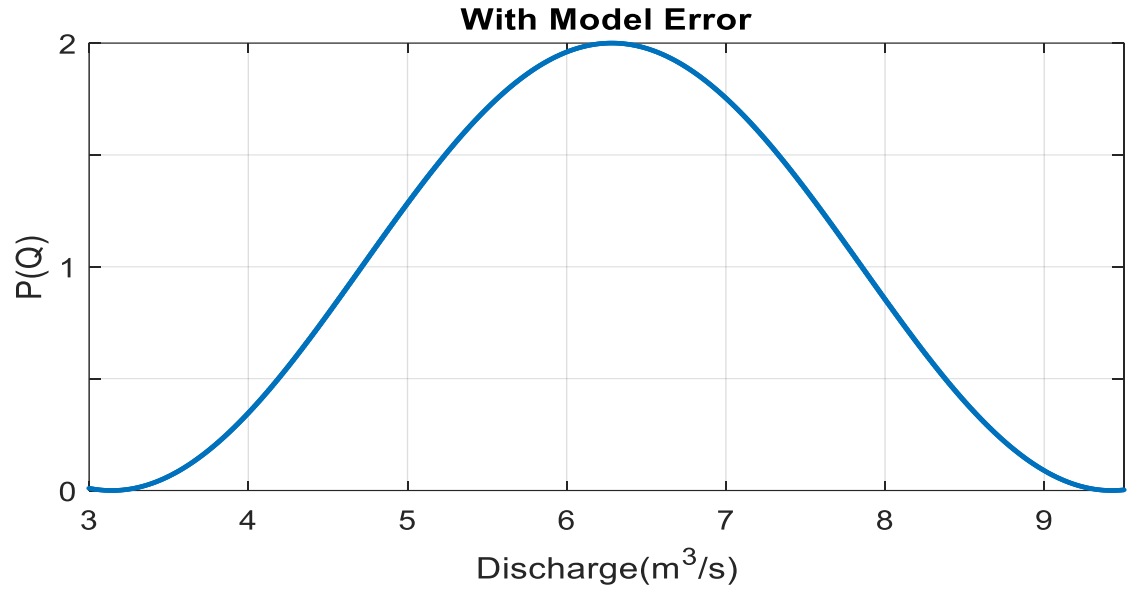

Figure 1.6: With Model Error

Figure 5.6 shows with model error in the rainfall-runoff region. Adding model errors widens the predictive distribution, and the posterior of τ shifts further increase model errors and

overlap with the likelihood function. The posterior of shifts in the proposed method maintains the formal wave form from discharge 0 m^3/s to 10 m^3/s. The posterior shift increases to maximum at 6.5 m^3/s. In the model with error, the obtained probability is 2 because of the ensemble Kalman Filter that filters the history of states rather than previous state.

Figure 5.7 shows the infiltration rate and runoff level of the proposed network, larger the rainfall intensity of 1.5cm/hr, the higher the initial and steady infiltration rates from 6 to 8, and the cumulative infiltration increased faster with time and the runoff level is from 0 to 0.5 cm. Infiltration rate increased due to the layers present in the proposed prophetic multilayer network which estimates infiltration rate using urban land cover model which does not separate the catchment for estimation.

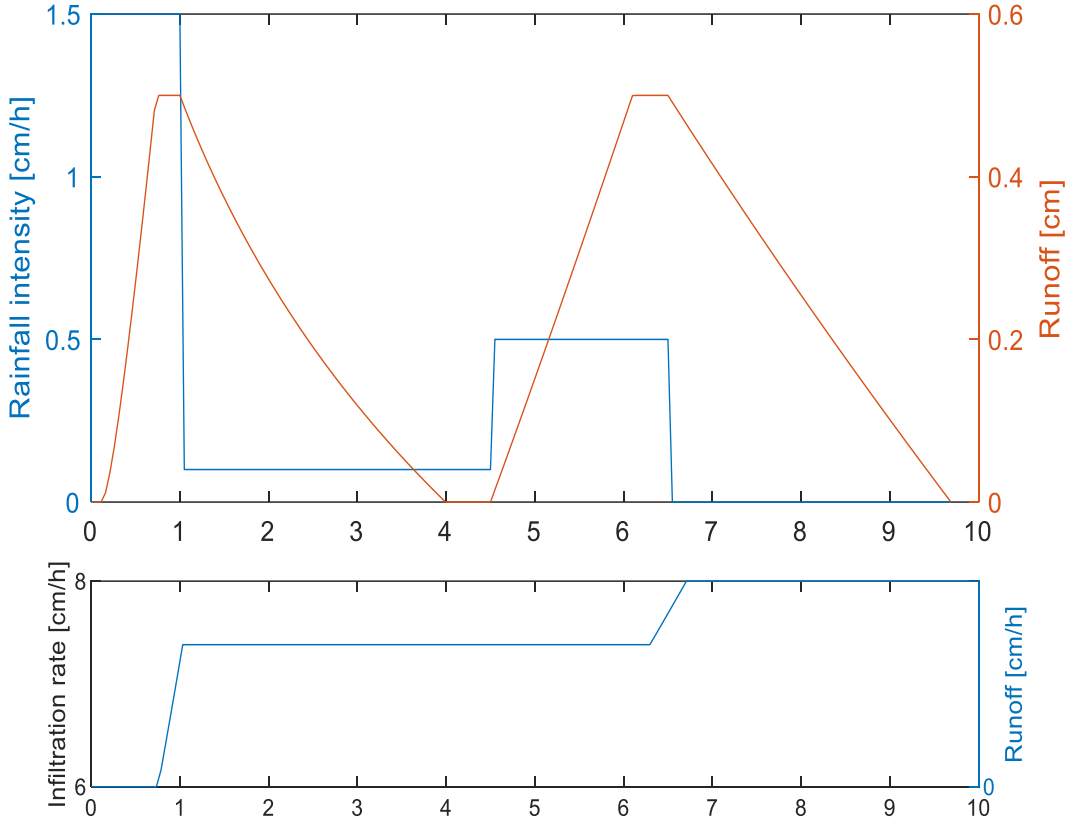

Figure 1.7: Infiltration Rate in Runoff

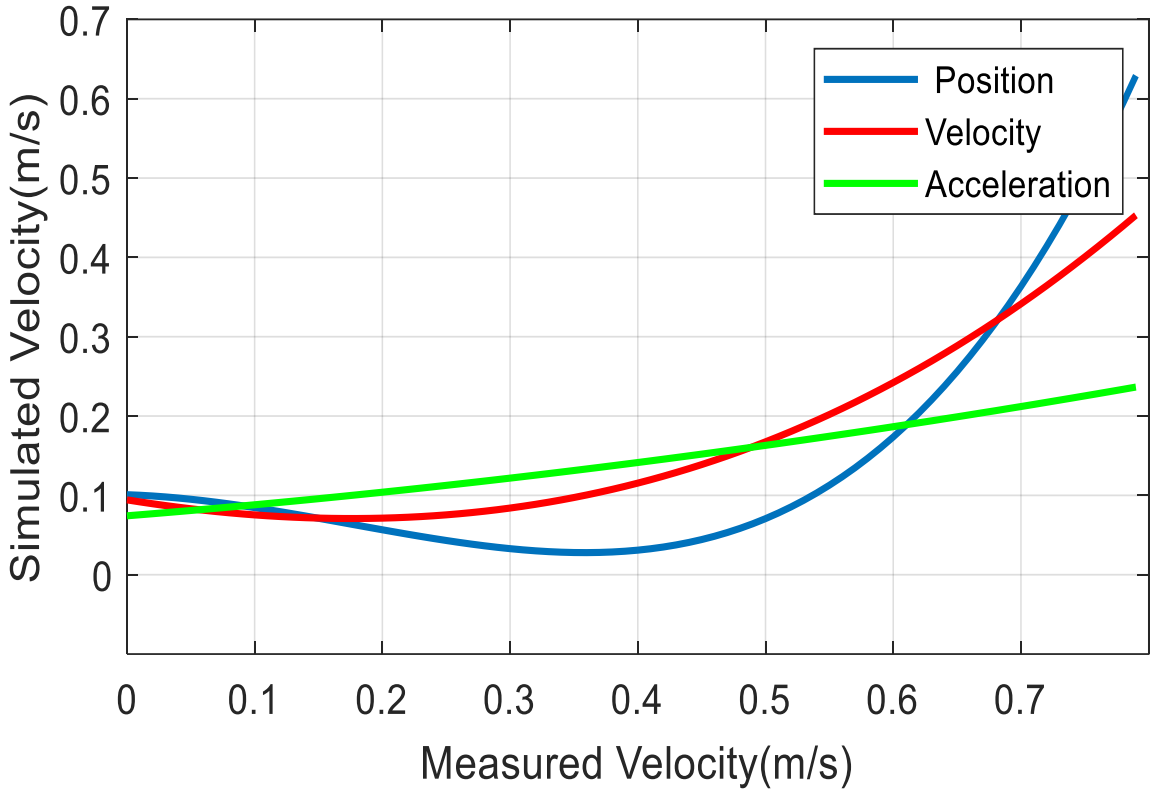

Figure 1.8: Simulated velocity

Figure 5.8 shows the measured velocity in terms of position, velocity, and acceleration by the well-ordered selective genetic algorithm. The genetic algorithm measures the velocity with bend areas thus avoiding the low depth steep slopes in the hill. The highest velocities are better represented by the model by 0.45 m/s. The highest velocity was obtained in the proposed method by using well order selective genetic algorithm for unstructured mesh which deals with arbitrary complex geometries.

1.3 Model Results Evaluation for HEC-HMS and RF model

There are many criteria selected to evaluate the prediction performance based on hydrological forecasting guidelines; according to these criteria, the best model for forecasting was chosen. In this research three statistical criteria are used, coefficient of determination (R^2), mean absolute error (MAE) and root mean square error (RMSE). The formulation can be expressed as equation 27,28 and 29 respectively. (Chai and Draxler,2014)

$$R^2 = \left(\frac{1}{n} \times \frac{\sum(x_i - \bar{x})(y_i - \bar{y})}{(\sigma_x)(\sigma_y)}\right)^2 \qquad \text{eq (27)}$$

$$RMSE = \sqrt{\frac{\sum_{i=1}^{n}(x_i - y_i)^2}{n}} \qquad \text{eq (28)}$$

$$MAE = \frac{1}{n}\sum_{i=1}^{n}|x_i - y_i| \quad \text{eq (29)}$$

Where n is the number of data, x and y are observed and estimated values, and σ_x and σ_y are the standard deviation of the observed and estimated data. It should be mentioned that low value (closer to zero) for the RMSE, while for R^2, a high value (closer to the unity) signifies that there is a good agreement between observed and modeled estimation data.

1.3.1 Results and Discussion for **HEC-HMS and RF model**

This study has used daily discharge, rainfall and temperature data from the M.H. Halli station in India. The basis for comparing a process-based model with a time series model lies in their respective approaches to modeling hydrological systems. A process-based model relies on a detailed representation of the physical and hydrological mechanisms governing the system, offering a comprehensive understanding of underlying processes but demanding substantial data and computational resources. In contrast, a time series model employs statistical techniques to analyze historical data patterns without explicit consideration of system processes, providing simplicity and adaptability but potentially oversimplifying complex dynamics. The choice between these models hinges on the specific objectives, data availability, and the balance between detailed process understanding and computational efficiency needed for accurate hydrological modeling. As stated earlier, two models, i.e., HEC-HMS and RF model have been developed for discharge forecasting. A general view of the study is given Figure 5.9.

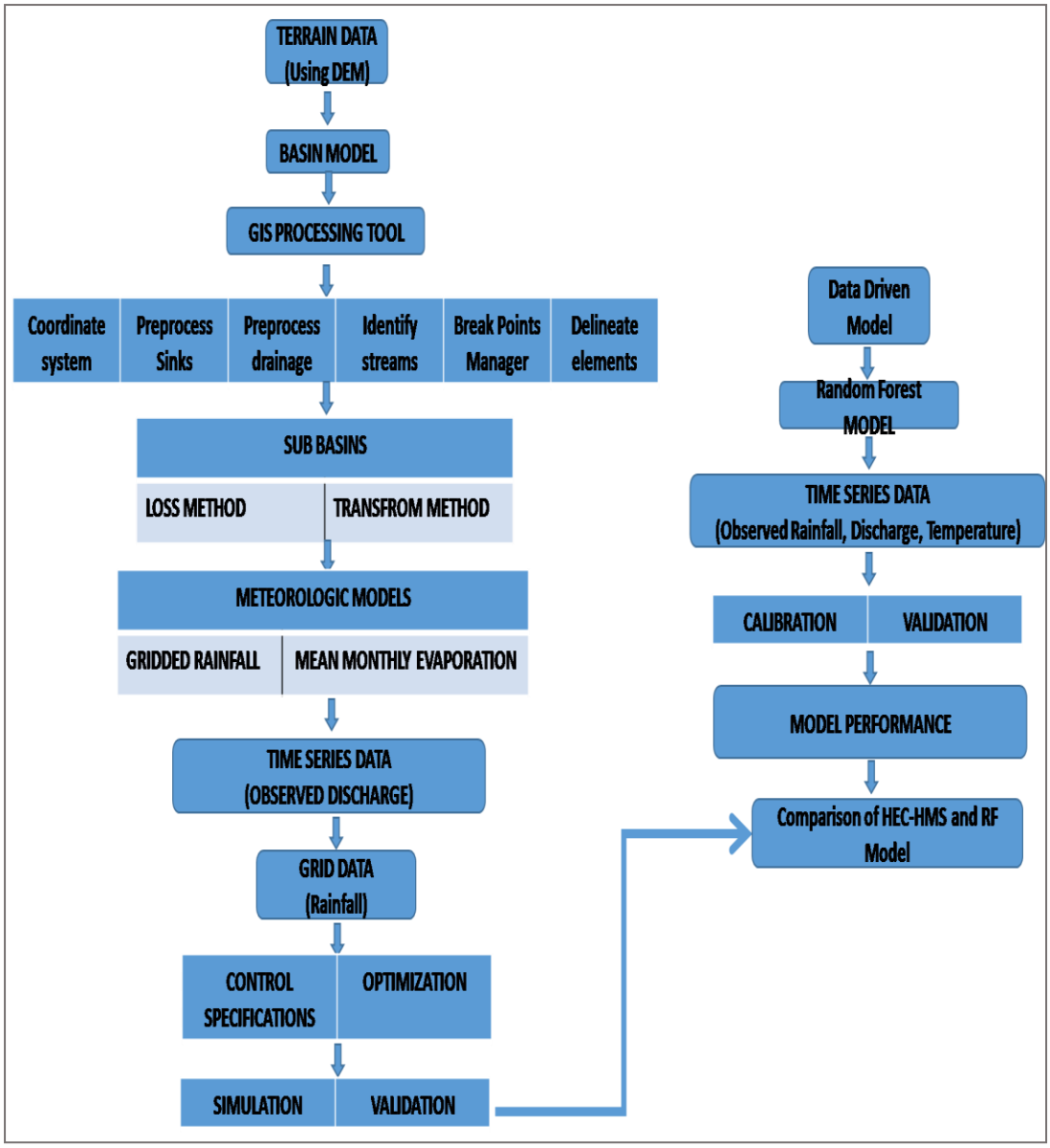

Figure 1.9: Flowchart of the modeling procedure

The basis for comparing a process-based model with a time series model lies in their respective approaches to modeling hydrological systems. A process-based model relies on a detailed representation of the physical and hydrological mechanisms governing the system, offering a comprehensive understanding of underlying processes but demanding substantial data and computational resources. In contrast, a time series model employs statistical techniques to analyze historical data patterns without explicit consideration of system processes, providing simplicity and adaptability but potentially oversimplifying complex dynamics. The choice between these models hinges on the specific objectives, data availability, and the balance between detailed process understanding and computational efficiency needed for accurate hydrological modeling.

1.3.2 Statistical Analysis of Data

Initially, daily discharge, rainfall and temperature data were divided into two parts i.e. calibration/training and validation/testing. Among entire data, 8 years data were selected for calibration and the remaining 7 years data were selected for testing the developed models. The statistical parameters for calibration/training and validation/testing of discharge, rainfall and temperature datasets were calculated as shown in Table 5.2.

Table 1.2: Statistics of the data

Dataset	Datatype	Data no.	Mean	STD	CV	Max	Min
Calibration (2003-2010)	Rainfall (mm)	1346	6.12	8.34	1.36	62.415	0.000
	Discharge (Cumec)		95.13	167.47	1.76	1203.000	0.023
	Temperature (^{0}C)		23.23	1.01	0.05	27.733	19.920
Validation (2010-2017)	Rainfall (mm)	1198	6.33	8.67	1.37	76.940	0.000
	Discharge (Cumec)		68.53	123.19	1.80	1102.000	0.040
	Temperature (^{0}C)		23.47	1.14	0.09	29.135	19.804

The coefficient of variance (CV) values for the rainfall, discharge and temperature testing/validation datasets were higher than those for the training/calibration, but, the mean and standard deviation values for discharge testing datasets were less than those for the training (Table 5.2). Furthermore, the maximum value of the discharge variable is higher during the training dataset. The maximum values for the rainfall and temperature testing dataset were higher than those for the training.

1.3.2.1 Discharge prediction with HEC-HMS hydrological model

The HEC-HMS hydrological model has been calibrated manually and automatically to optimize to obtain the best possible option fit. Initial deficit constant loss, Snyder unit hydrograph transform, and recession base flow method used. The calibration and validation performance of the HEC-HMS 4.7 is carried out by comparing of the daily simulated discharge with the observed discharge at the M.H. Halli station. To assess the performance of the model predictability of representing the hydrological simulation of the reality of the basin. Four basic statistical hydrological model performance check used. The R^2 (relation coefficient), MAE (mean absolute error) and RMSE (root mean square error).

1.3.2.2 Model Calibration

The model for MH Halli station is calibrated using 2003 to 2010 daily rainfall, temperature and discharge data. Manual and automatic calibration techniques are applied to estimate values of parameters. The sub basins are assumed to be homogenous and the model parameters are assigned according to the type of soil and land use pattern within sub-basin. The optimal values of the model parameters are obtained using the criterion of maximizing the efficiency by comparing the observed and simulated flows. The accuracy of the model is verified by qualitative and quantitative analysis.

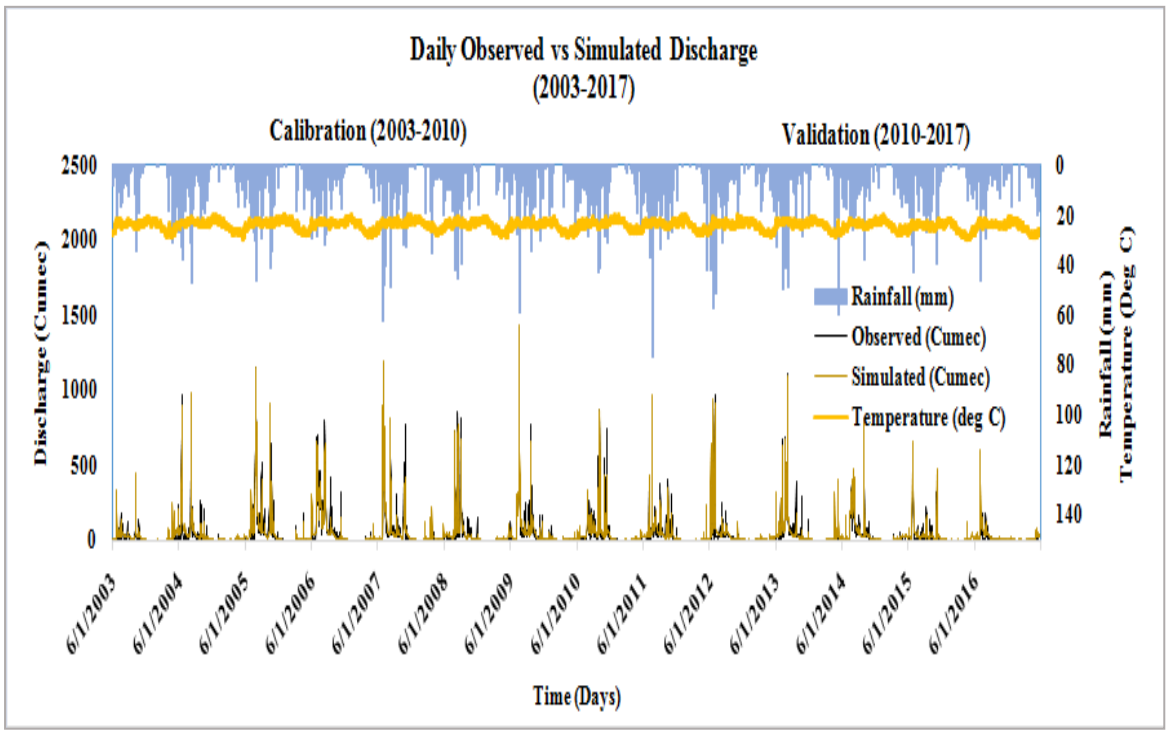

Figure 1.10: HEC-HMS model performances in terms of comparison of observed and simulated discharge

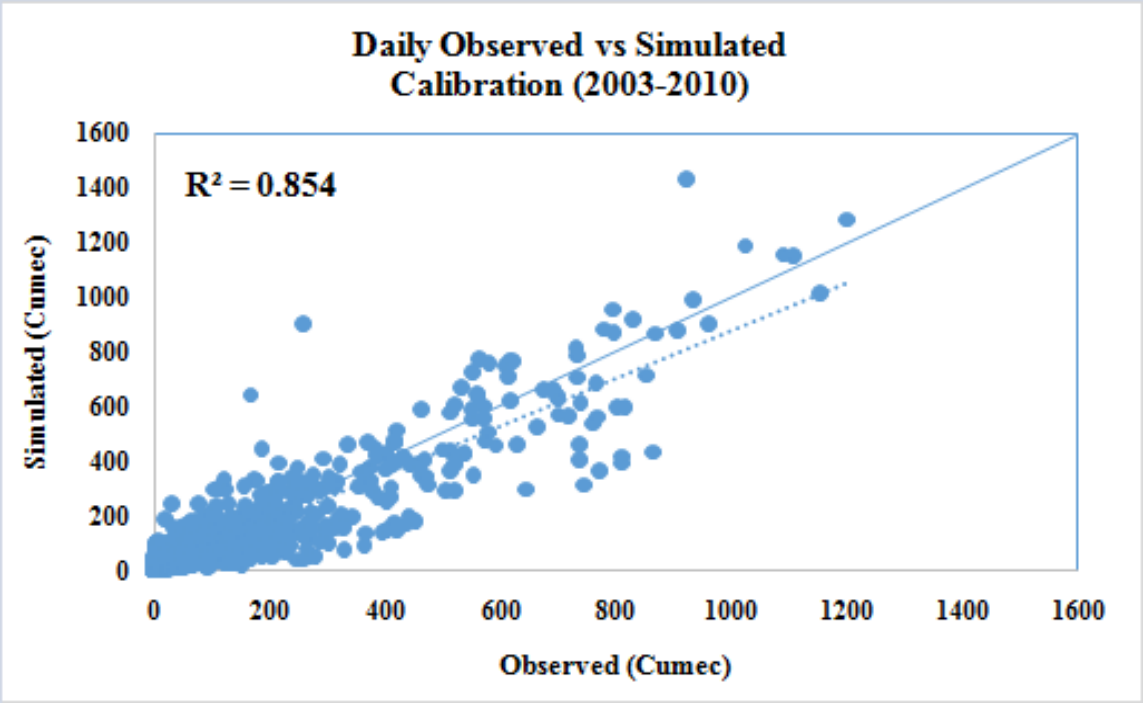

Figure 1.11: HEC-HMS model scatter plot between observed vs simulated discharge during calibration

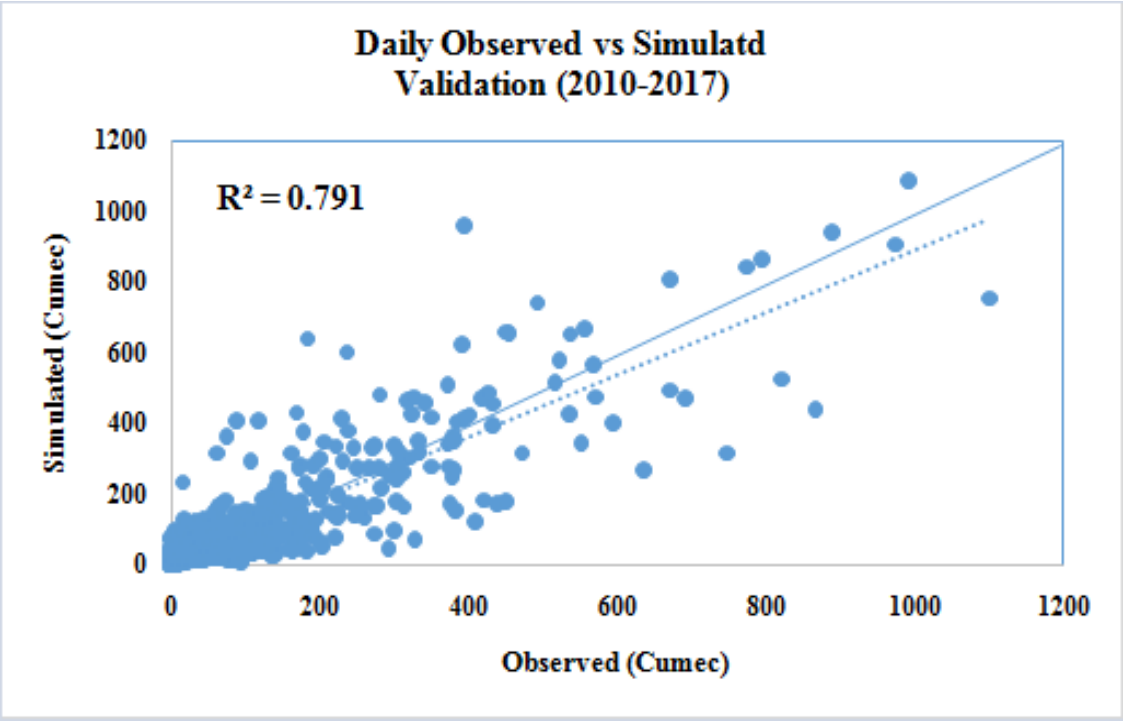

Figure 1.12: HEC-HMS model scatter plot between observed vs simulated discharge during validation stage

The simulated and observed discharge time series (figure 5.11 and 5.12) and scatter plot at calibration period 2003 to 2010 is shown in Figure 5.11. It is seen that the daily hydrograph of the simulated discharge caught the observed discharge during calibration period (2003-

2010). However, the peak value of the simulated discharge is under predicted in the model as compared to the observed discharge of the outlet station. From the statistical analysis (Table 5.2) the coefficient of determination (R^2) has calculate as 0.854. Which shows the developed hydrological model for the MH Halli station is well performing for calibration period. Manual and automatic method was applied for the optimization of model parameter during calibration and validation period.

1.3.2.3 Model Validation

The validated result of the HEC-HMS model for MH Halli station can be seen in the Figure 4-5. Based on the calibrated parameters and values the model is validated from (2010 – 2017), and the performance a little bit improved. The daily hydrograph well simulated with observed discharge flow. From the statistical analysis (Table 5.2) the coefficient of determination (R^2) has calculate as 0.791. Which shows the developed hydrological model for the MH Halli station is well performing for calibration period. However as like calibration period, there is also under prediction in the peak flow.

1.3.3 Discharge prediction with RF model

Table 5.3 appears the RF prediction performance using the best predictive variables based on the R^2, RMSE, and MAE for the calibration. Figure 5.13,5.14 and 5.15 delineates the performance of the RF models. As shown in Table 5.3, the range of R^2 for the predicting discharge in all scenarios was highly correlated (R^2= 0.974 - 0.994) in training phase. According to the R^2 values, the RF model from the second scenario produced the best performance during training (0.994), followed by the first scenario. R^2 is susceptible to outliers and should not be used entirely for evaluating generated models because it is optimized for differences between the mean and variance of measured and expected quantities (Legates and McCabe 1999; Shiri and Kisi 2012). As a result, alternative error measurement indices were employed to assess the performance of the model. Based on RMSE and MAE, the RF (2^{nd} scenario) was superior to the other types. The training phase rather than the testing phase yields superior results for the effectiveness of RF (2^{nd} scenario). For instance, the MAE and RMSE indices during the training stage were 0.166 and 12.61, respectively. Each tree in RF regression trees is created separately on a bootstrap sample. As a result, they are only weakly connected. The risk of over fitting the training data set was reduced as a result. Furthermore, it was discovered that the RF algorithm could nearly formulate the data trend, that the model could

accurately give the rainfall prediction, and that the predicted and observed values were nearly identical.

Table 1.3: Comparison of HEC-HMS and Random Forest models in terms of R^2, RMSE, and MAE

Models	Calibration			Validation		
	R^2	RMSE	MAE	R^2	RMSE	MAE
HEC-HMS	0.854	49.59	22.03	0.791	41.64	16.85
Data Driven model (Random Forest)						
Rain, Temp, Discharge (1^{st} scenario)	0.974	29.02	0.418	0.189	88.12	25.29
Rain, Temp, D-1, D-2 (2^{nd} scenario)	0.994	12.61	0.166	0.325	87.85	25.15

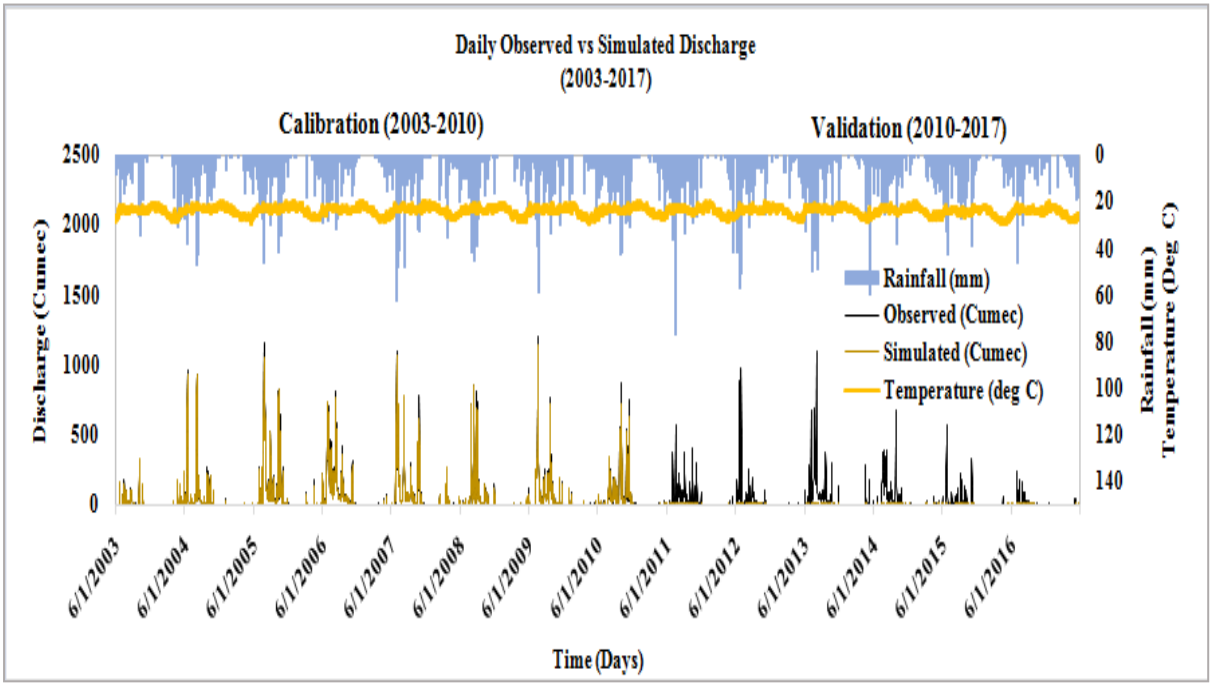

Figure 1.13: RF model performances in terms of comparison of observed and simulated discharge

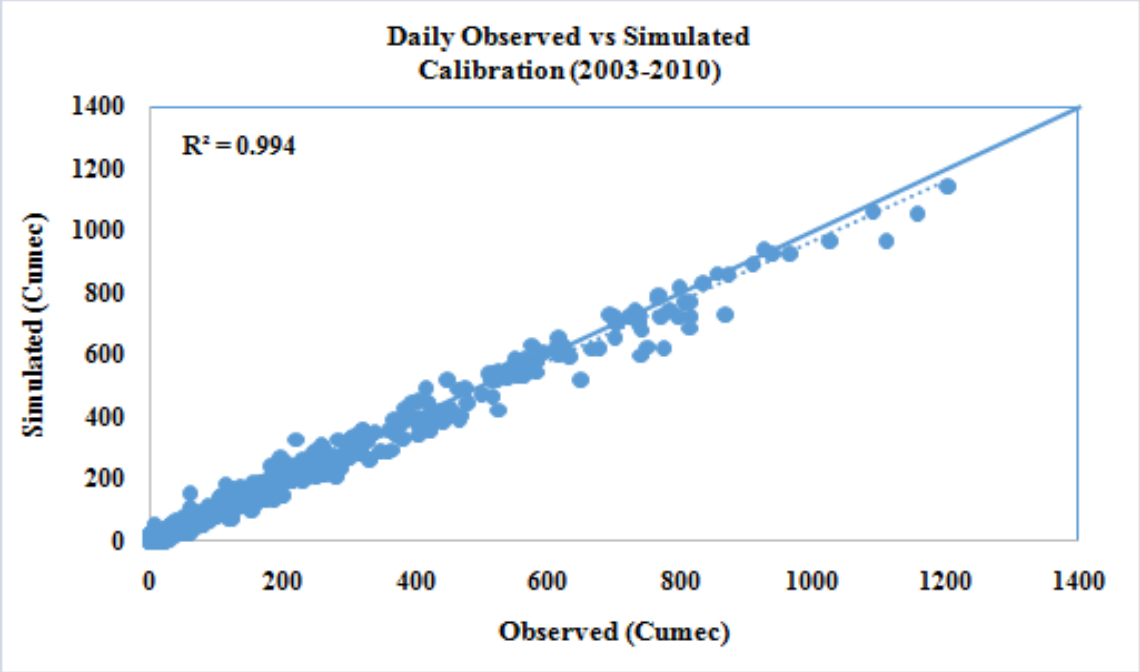

Figure 1.14: RF model scatter plot between observed vs simulated discharge during calibration stage

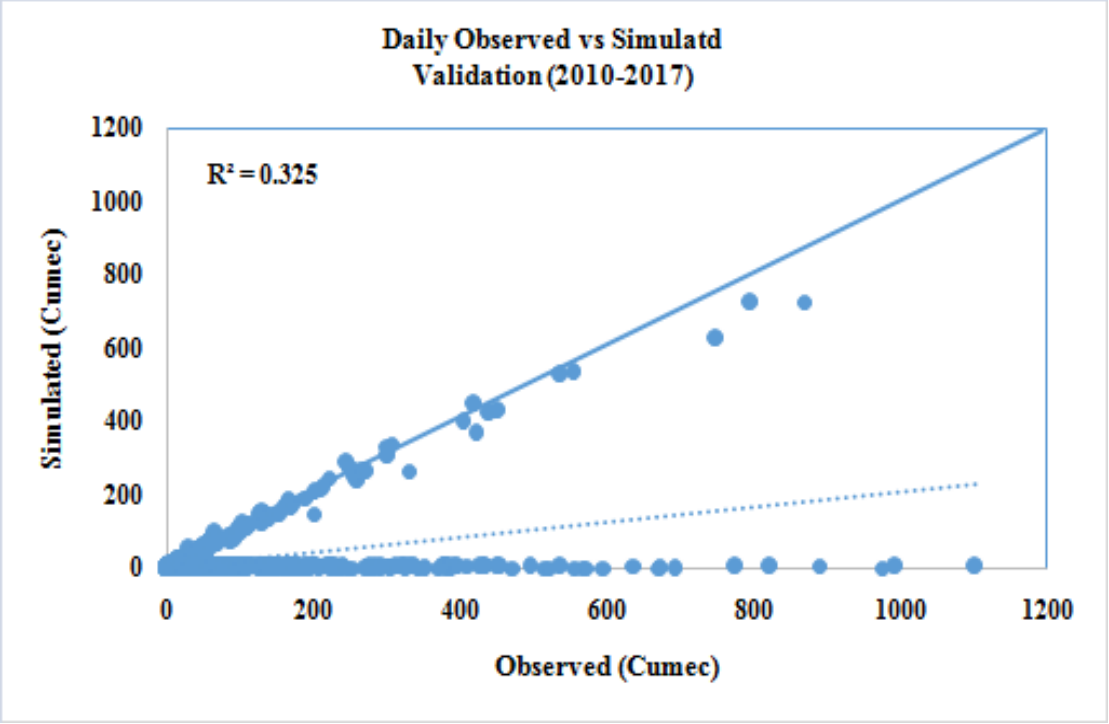

Figure 1.15: RF model scatter plot between observed vs simulated discharge during validation stage

1.3.4 Comparison of Prediction Models (HEC-HMS and Random Forest)

The ability of the HEC-HMS model for runoff prediction was investigated and compared with RF model. The accuracies of the HEC-HMS and RF models were compared using R^2, MAE and RMSE. Table 5.3 presents the training and testing results of the MH Halli station. In Table 5.3, it is shown that HEC-HMS model acquired the best R^2, MAE and RMSE in the training and testing stages. Figure 5.16 delineate the comparison of HEC-HMS and RF model. The HEC-HMS model considerably improved the accuracy with respect to RF model in the testing stage. Results indicated that the HEC-HMS model might provide an alternative to the RF models for predicting runoff.

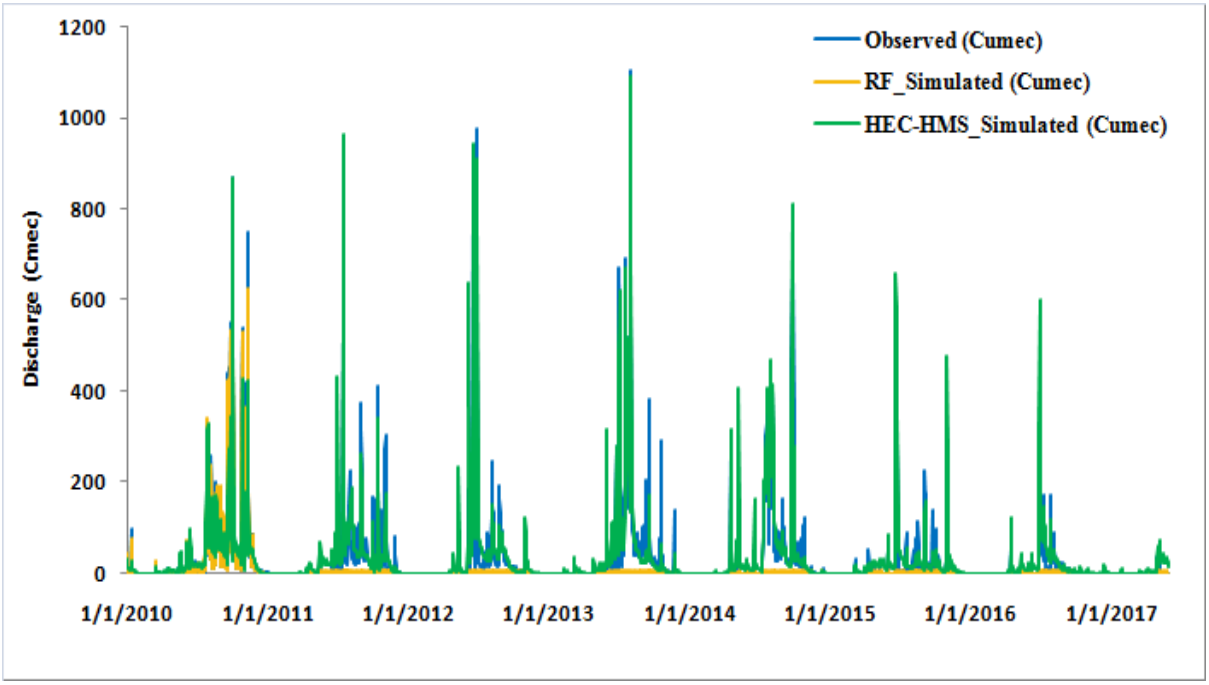

Figure 1.16: Comparison of HEC-HMS and RF model

1.4 Model Results Evaluation for SWAT and M5P Model

For the best forecasting model, a number of criteria were developed to evaluate the prediction performance based on hydrological forecasting standards. Three statistical measures—the coefficient of determination (R^2), the indicator of agreement (d), the Nash-Sutcliffe efficiency (NSE), and the root mean square error (RMSE) are employed in this study. The formulation can be expressed as equation 30,31,32 and 33 respectively:

$$R^2 = \left(\frac{1}{n} \times \frac{\sum(x_i - \bar{x})(y_i - \bar{y})}{(\sigma_x)(\sigma_y)}\right)^2 \qquad \text{eq (30)}$$

$$RMSE = \sqrt{\frac{\sum_{i=1}^{n}(x_i - y_i)^2}{n}} \quad \text{eq (31)}$$

$$d = 1 - \frac{\sum_{i=1}^{n}(x_i - y_i)^2}{\sum_{i=1}^{n}(|y_i - \bar{x}| + |x_i - \bar{x}|)^2} \quad \text{eq (32)}$$

$$NSE = 1 - \frac{\sum_{i=1}^{n}(x_i - y_i)^2}{\sum_{i=1}^{n}(x_i - \bar{x})^2} \quad \text{eq (33)}$$

Where n is the number of data, x and y are observed and estimated values, and σ_x and σ_y are the standard deviation of the observed and estimated data. It should be mentioned that low value (closer to zero) for the RMSE, while for d and R^2, a high value (closer to the unity) signifies that there is a good agreement between observed and modeled estimation data.

1.4.1 Results and Discussion for SWAT and M5P model

This study has used daily discharge, rainfall and temperature data from the M.H. Halli station in India. As stated earlier, two models, i.e., SWAT and M5P have been developed for discharge forecasting. A general view of the study is given Figure 5.17.

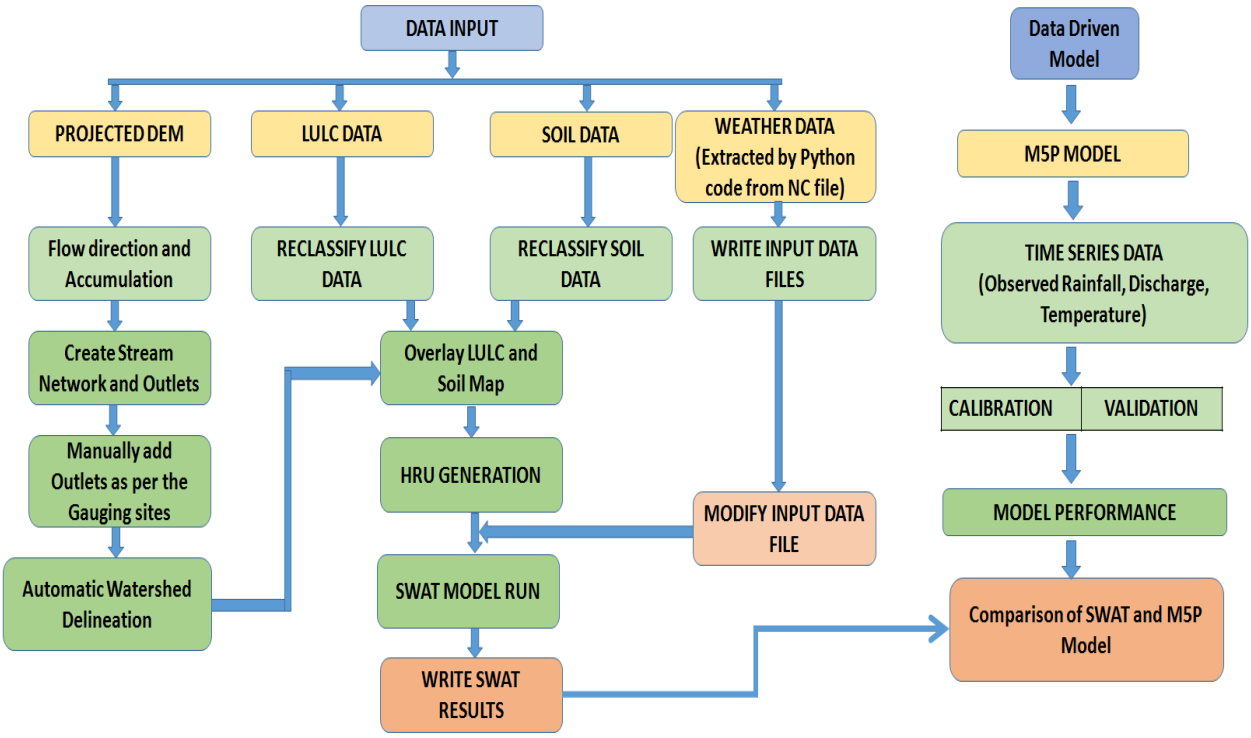

Figure 1.17: Flowchart of the modeling procedure (SWAT and M5P)

1.4.2 Statistical Analysis of Data

Daily data on discharge, precipitation, and temperature were first split into two categories: calibration/training and validation/testing. Eight years' worth of data were chosen from the total

for calibration, and the remaining seven years' worth were chosen for testing the constructed models. The statistical parameters for the discharge, rainfall, and temperature datasets' calibration, training, validation, and testing were computed as given in Table 5.2.

Although the mean and standard deviation for the discharge testing datasets were lower than those for the training, the coefficient of variation (CV) values for the temperature, discharge, and rainfall testing/validation datasets were higher than those for the training (Table 5.2). Additionally, the training dataset has a higher maximum value for the discharge variable. The maximum values in the testing dataset for temperature and rainfall were higher than those in the training dataset.

1.4.3 Discharge prediction with SWAT hydrological model

1.4.3.1 Model Application

In fact, the simulation process, which is used to estimate model expectation results, is not possible without model calibration and validation. Because of the lack water quality data to make a comparison, the model was simply calibrated and validated against monthly flow measurements to better depict the water cycle. The model directly replicated the sediment observations. From 2003 to 2017, flow measurements are available. Because it was close to the time that satellite photos had been used to specialise the cultural progress and because it offered seven years prior to the calibration, from 2003 to 2010, the period 2010–2017 was chosen for validation.

1.4.3.2 Model Calibration

The model was calibrated using monthly flow records to further the calibration for the entire basin. At fact, over a period of 7 years, the SWAT model in the MH Halli station was calibrated by contrasting the measured discharges with the simulated discharges in the hydrometric station under consideration. The comparison study demonstrates a reasonable level of sufficiency. The results of the model accuracy evaluation have suggested that the overall values of R^2 is within the criteria " very good" (0.94), NSE is "very good" (0.88) (88% of the simulated discharges are similar to the discharges observed) and RMSE and d is “good” (47.71 and 0.98). For compatibility between the model results and the actual observed values of discharge at the MH Halli Station, the daily hydrograph is shown in Figure 5.18, 5.19 and 5.20 respectively. The results indicated that the SWAT model can be applied to assess discharge with acceptable accuracy.

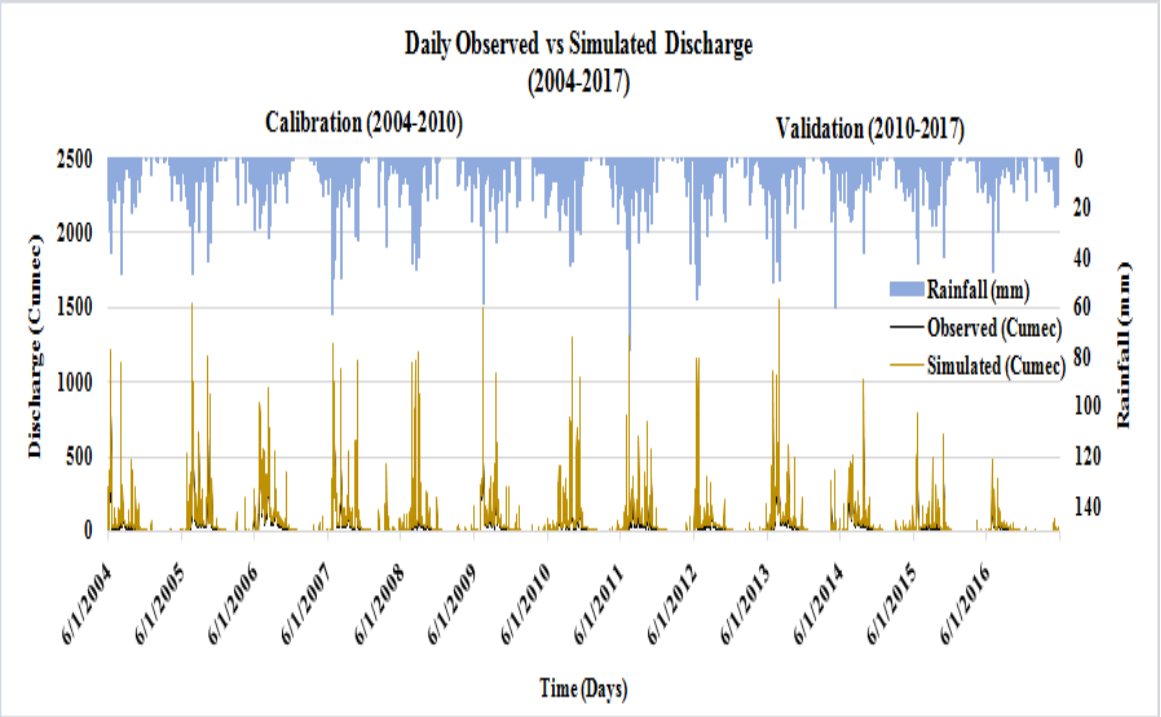

Figure 1.18: SWAT model performances in terms of comparison of observed and simulated discharge

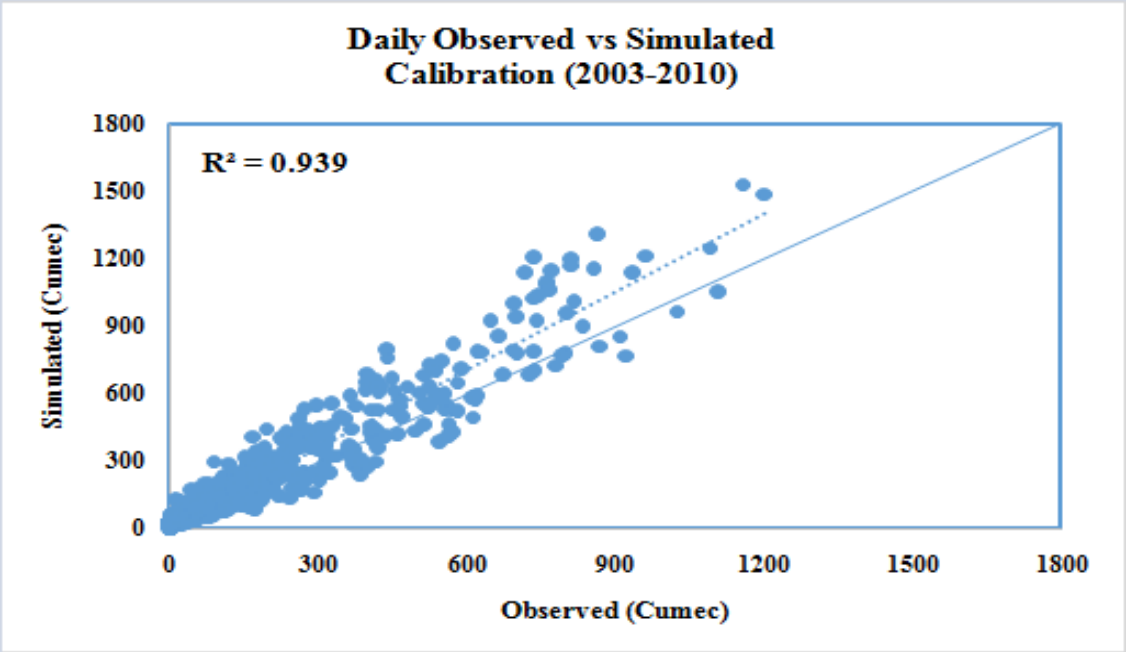

Figure 1.19: SWAT model scatter plot between observed vs simulated discharge during calibration stage

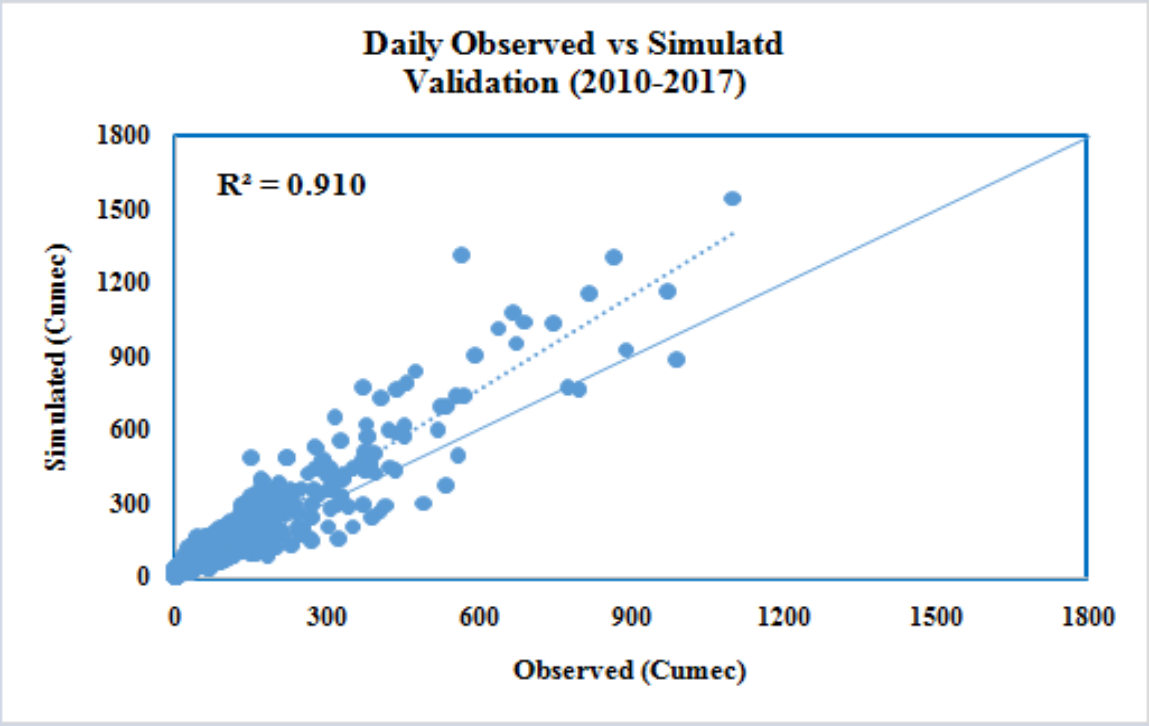

Figure 1.20: SWAT model scatter plot between observed vs simulated discharge during validation stage

1.4.3.3 Model Validation

By comparing the discharges of the measured flow to the simulated flow in the hydrometric station under consideration, SWAT model validation was carried out over additional periods of the dataset. The validation enabled us to acquire a good model performance for discharges with RMSE and d are respectively 50.54 and 0.95, in accordance with the performance assessment criteria of the model advised for a monthly time step (Moriasi et al., 2007). The NSE and R^2 threshold is 0.74 and 0.91, and it also assesses the relationship between the two statistical series. The good model calibration and capacity to accurately reflect various climatic scenarios is also demonstrated by the good agreement between simulations and observations throughout the validation process.

The sensitivity analysis for the SWAT model was not conducted in this study. The rationale behind this decision lies in the satisfactory performance observed during the initial simulation. As the results met the predefined criteria, it was determined that the model had been appropriately configured during the setup phase. The understanding of the physical meaning of all input parameters, as emphasized in the methodology section, played a crucial role in achieving these satisfactory results. Therefore, in the context of this study area and model setup,

a sensitivity analysis was deemed unnecessary, given the confidence in the accuracy of the initial simulation outputs.

1.5 Discharge prediction with M5P model

Weka software was used to build the M5P model tree. The user-defined parameter (M) had the best values of 4. As mentioned, prior, training and testing dataset were randomly selected from the 50-50 split. This algorithm results were then evaluated using R^2, RMSE, NSE and d. The fitting accuracy of the used models for each input composition over the training phase is summarized in Table 5.4. As appeared in Table 5.4, the efficiency fluctuated from one compound to another. The primary reasons for the oscillation are the differences between the effects of each selected input variable on the stream flow prediction. According to Table 2, the best correlation coefficient to estimate discharge in training data was 0.97 for 2nd scenarios.

Figure 5.21 delineates the performance of the M5P models. Table 5.4 shows the effects of the M5P approach in terms of R^2, RMSE, NSE and d for both (calibration and validation) phases. According to Table 5.4, the performance criteria for the scenario 2 are $R^2 = 0.97$, RMSE = 29.12, NSE = 0.91 and d = 0.99 in calibration stage, while the performance criteria for the scenario 2 are $R^2 = 0.92$, RMSE = 37.02, NSE= 0.76 and d = 0.96 in validation stage. Figure 5.22 and 5.23 shown the M5P model scatter plot between observed and simulated discharge during calibration and validation stage.

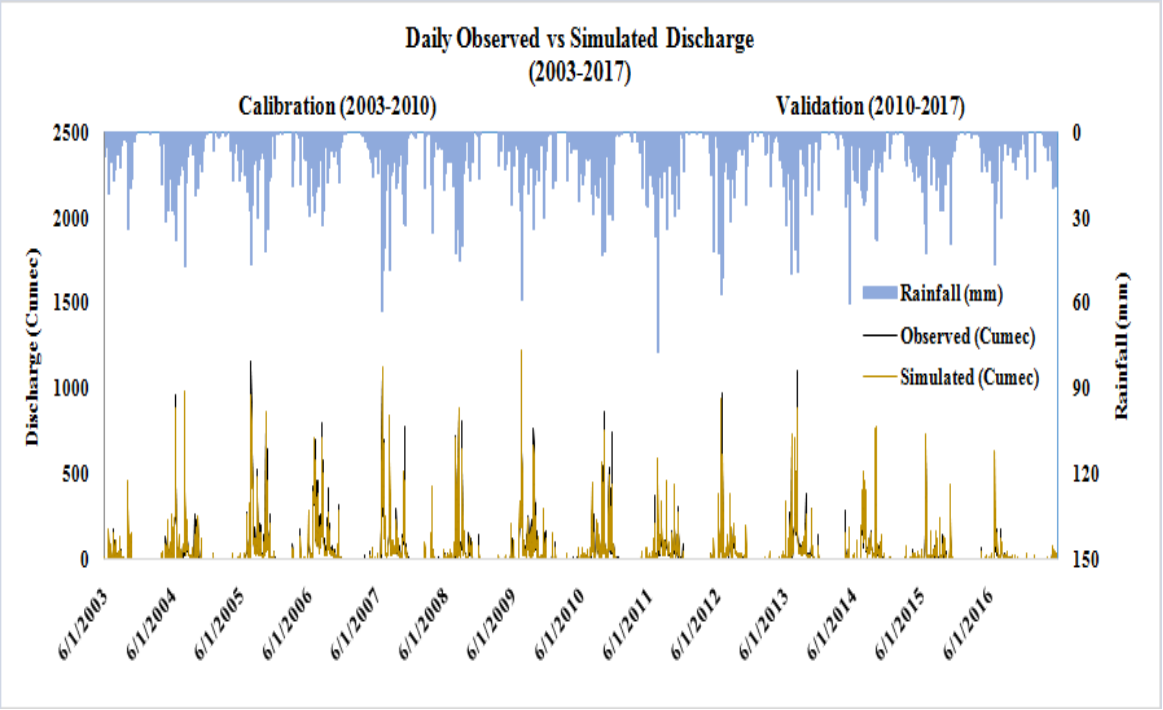

Figure 1.21: M5P model performances in terms of comparison of observed and simulated discharge

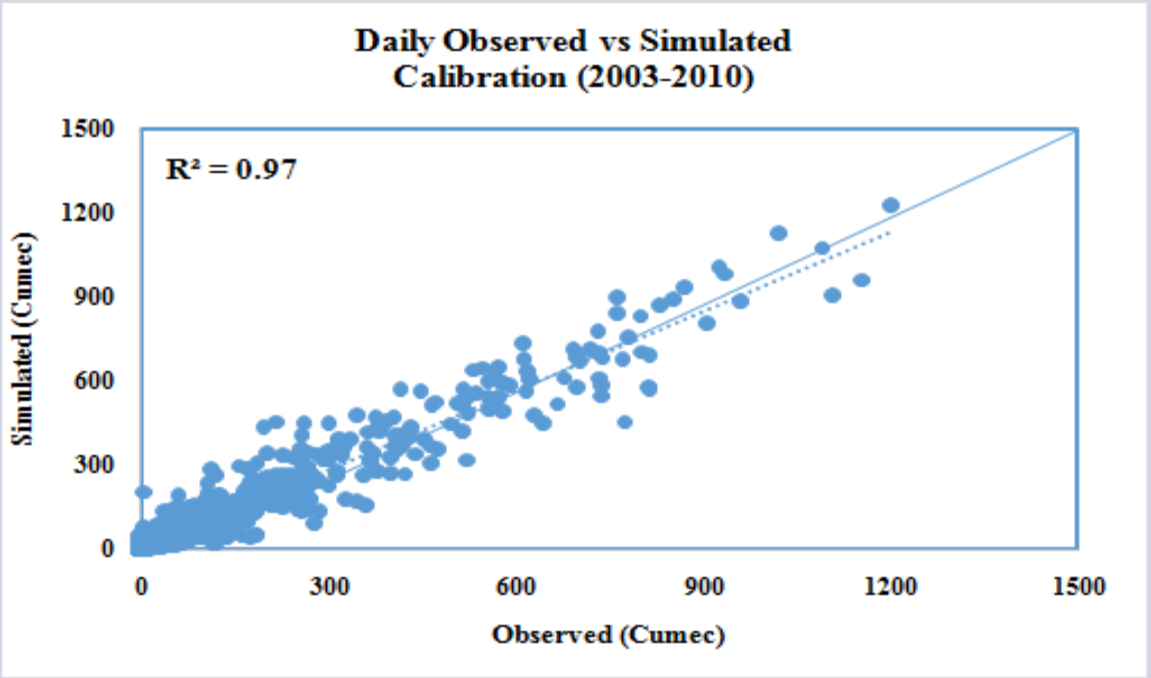

Figure 1.22: M5P model scatter plot between observed vs simulated discharge during calibration stage

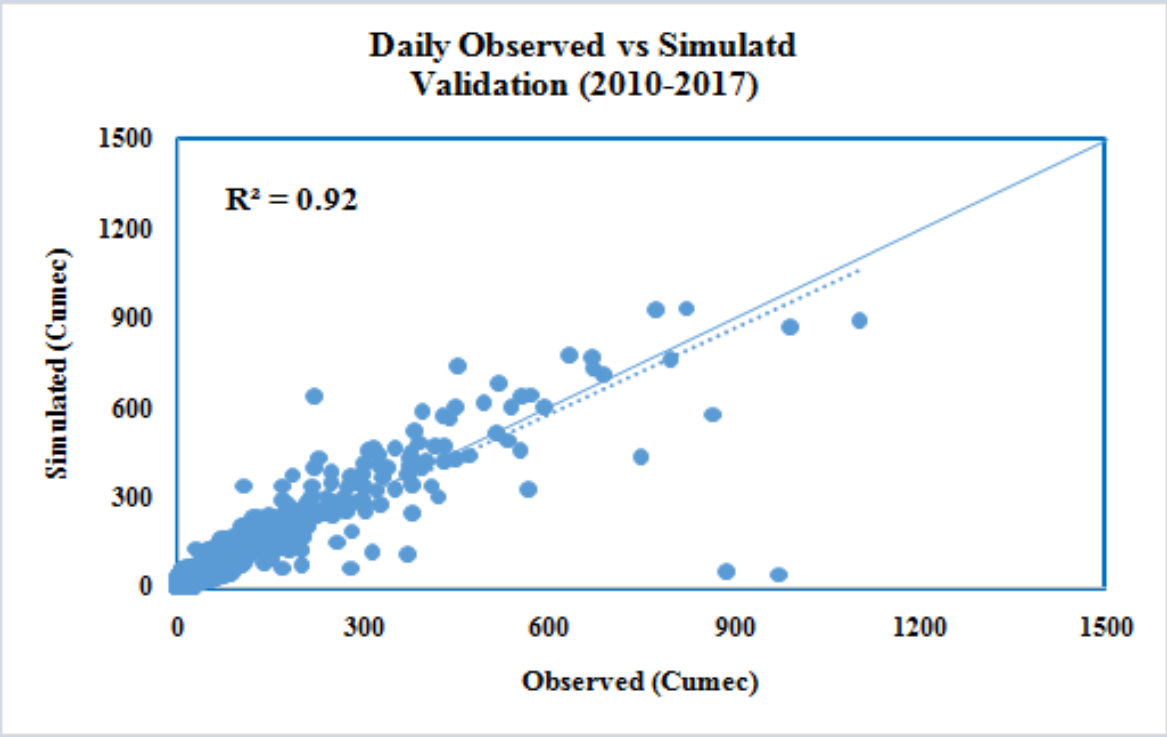

Figure 1.23: M5P model scatter plot between observed vs simulated discharge during validation stage

According to the R^2 values, the RF model from the second scenario produced the best performance during calibration, followed by the first scenario. Because R^2 is tuned for differences between the mean and variance of measured and expected quantities, it is vulnerable to outliers and should not be used only for evaluating created models (Legates and McCabe, 1999; Shiri and Kisi, 2012). As a result, different error measurement indices were used to evaluate the model's performance. Based on RMSE, NSE and d, the M5P (2^{nd} scenario) was superior to the other types.

Table 1.4: Comparison of SWAT and M5P models in terms of R^2, RMSE, NSE and d

Models	**Calibration**				**Validation**			
	R^2	**RMSE**	**NSE**	**d**	**R^2**	**RMSE**	**NSE**	**d**
SWAT	0.94	47.71	0.88	0.98	0.91	50.54	0.74	0.95
Data Driven model								
Rain, Temp, Discharge (1^{st} scenario)	0.81	73.00	0.75	0.86	0.79	60.34	0.63	0.84
Rain, Temp, D-1, D-2 (2^{nd} scenario)	0.97	29.12	0.91	0.99	0.92	37.02	0.76	0.96

1.6 Comparison of Prediction Models (SWAT and M5P)

Our investigation centered on assessing the predictive capabilities of the SWAT model in contrast to the M5P model, with a focus on their effectiveness in predicting runoff. To accomplish this, we employed several evaluation metrics, including R^2, RMSE, NSE, and d, to thoroughly compare the performance of both models.

The outcomes of this analysis for the MH Halli station are presented in Table 5.4, offering a comprehensive overview of the models' performance during both the training and testing phases. Table 5.4 reveals that the M5P model consistently outperformed the SWAT model across all evaluation metrics, indicating its superior predictive accuracy.

Specifically, during the calibration and validation phases, the M5P model achieved the highest R^2, signifying a stronger linear relationship between predicted and observed values. Additionally, the M5P model exhibited the lowest RMSE (Root Mean Square Error), indicating smaller prediction errors, and the highest NSE (Nash-Sutcliffe Efficiency), signifying better model efficiency in reproducing observed runoff patterns. The coefficient "d" also favored the M5P model, suggesting a closer alignment between predicted and observed runoff.

Figure 5.24 graphically illustrates the performance comparison between the SWAT and M5P models, providing a visual representation of their respective strengths and weaknesses. Notably, the M5P model consistently outperformed the SWAT model across various scenarios and data points, highlighting its overall superiority in predicting runoff.

The decisive turning point in our evaluation occurred during the testing phase, where the M5P model's accuracy stood out significantly. It demonstrated remarkable proficiency in predicting runoff, showcasing its potential to serve as a viable substitute for the SWAT model in this application.

Based on these compelling results, it can be concluded that the M5P model holds great promise as an alternative to the SWAT model for accurate runoff prediction. This finding suggests that researchers and practitioners in the field of hydrology and water resource management may benefit from considering the M5P model as a valuable tool for their predictive modeling endeavors.

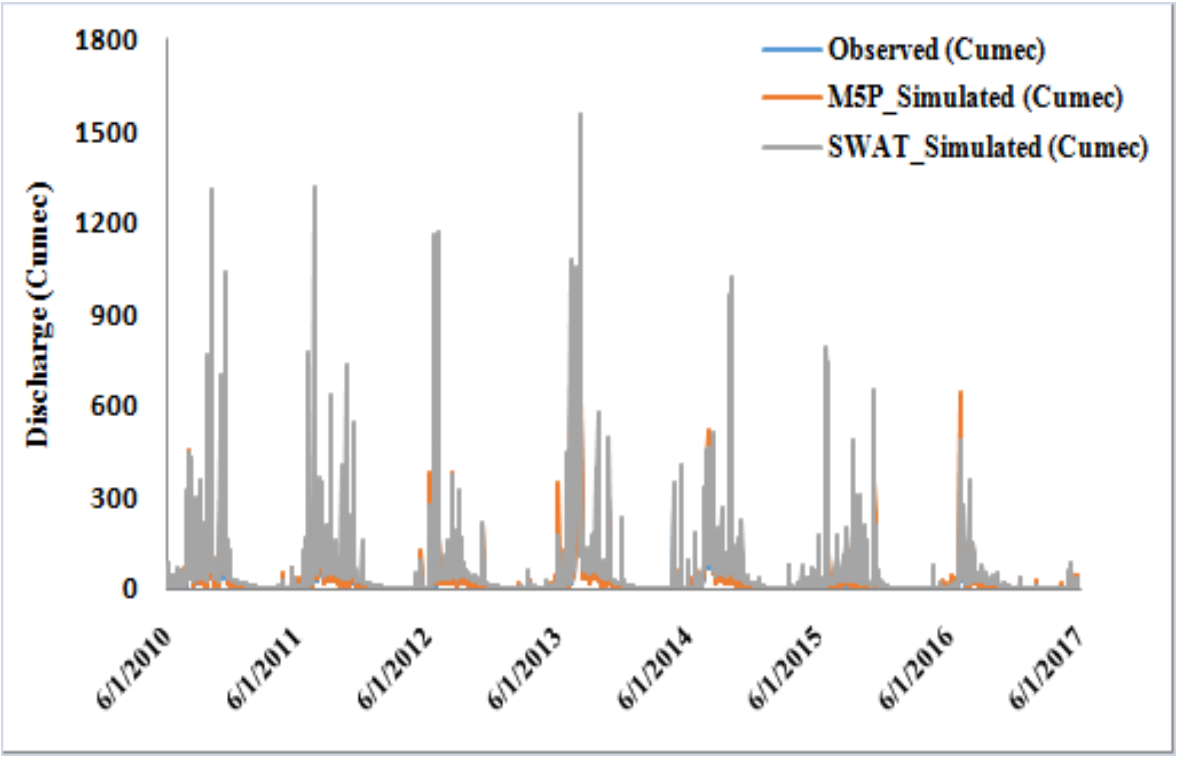

Figure 1.24: Comparison of SWAT and M5P model

The next chapter discusses the conclusion of results of simulation as well as discharge prediction model. Section 5.7 provides a summary of the chapter. The next section provides the summary of the chapter.

1.7 Summary

In this chapter, presented thesis effectively introduced a rainfall prognostic artificial model framework for the prediction of rainfall. The framework applied a posterior fire-breathing network to estimate model errors with random noise to reduce the uncertainty. Further, to regulate the infiltration rate, the system suggested a prophetic multilayer network that analyses the runoff levels with the soil moisture in urban and rural areas. In addition, to tackle the numerical challenge, the model integrates a well-ordered selective genetic algorithm to forecast different bend zones at low water depths on steep slopes. As a result of the rainfall model, everyday rainfall can be accurately anticipated to avoid environmental problems. Experimental findings demonstrate its superiority over existing runoff models, boasting a 1.5cm/hr infiltration rate, 0.05cm runoff level, and a 0.45mm achieved velocity. Additionally, it achieves the broadest prediction range of 12-20 mm, supported by subjective results.

Also, thesis presented a comprehensive discussion of the results and analyses derived from two distinct approaches: hydrological modeling, encompassing the use of HEC-HMS and SWAT

models, and soft computing techniques, where it has been employed Random Forest (RF) and M5P models. Our primary objective is to provide a thorough examination of the outcomes obtained from these diverse methodologies, shedding light on their strengths, weaknesses, and comparative performance. As a result, The HEC-HMS model provided the highest R2 in the calibration dataset and the lowest MAE and RMSE in validation data sets. Where the calculated value of R2 has found 0.854 for calibration period and 0.791 for validation period.The results of the SWAT model accuracy evaluation has suggested that the overall values of R2 is within the criteria " very good" (0.94), NSE is "very good" (0.88) (88% of the simulated discharges are similar to the discharges observed) and RMSE and d is "good" (47.71 and 0.98) during the calibration dataset.

First and foremost, embarked on the journey of hydrological modeling using the HEC-HMS and SWAT models, which are renowned for their utility in simulating and forecasting hydrological processes. These models were applied to our study area, where the extensive data on various hydrological variables, including precipitation, temperature, land use, and topography have been collected. The subsequent analysis of these models revealed critical insights into their efficacy in predicting runoff, streamflow, and other hydrological phenomena. Simultaneously, an attempt was made in the realm of soft computing techniques, harnessing the power of Random Forest and M5P models. These machine learning-based models are widely used for their adaptability and ability to capture complex relationships within datasets. The major aim of employing these models was to evaluate their predictive capabilities in comparison to the traditional hydrological models. As a result,The M5P model provided the highest R2, NSE and d and lowest RMSE in the calibration dataset. The RF model provided highest R2 and lowest RMSE and MAE in the calibration dataset.The M5P and RF both models performed outstanding during the calibration dataset with (R2=0.97, NSE=0.91, d=0.99 and RMSE= 29.12) and (R2=0.99, MAE=0.16, and RMSE= 12.61) than the validation dataset (R2=0.92, NSE=0.76, d=0.96 and RMSE= 37.02) and (R2=0.32, MAE=25.15, and RMSE= 87.85) correspondingly.

To facilitate a comprehensive assessment, a rigorous examination was conducted on the obtained results from the SWAT and M5P models, as well as the HEC-HMS and Random Forest model. A suite of evaluation metrics, including R^2, RMSE, NSE, and d, to quantify the accuracy and reliability of each model's predictions have been utilized. These metrics allowed

us to gauge the models' performance in terms of their ability to reproduce observed hydrological patterns and trends.

In particular, a direct comparison has been carried out between the SWAT and M5P models, as well as between the HEC-HMS and Random Forest model. This comparative analysis provided valuable insights into the relative merits of traditional hydrological modeling approaches versus machine learning-based techniques. It allowed us to discern which model or combination of models yielded superior results in terms of accuracy, precision, and robustness in predicting hydrological outcomes.

In this chapter, the reader will gain a deep understanding of the intricacies of hydrological modeling and soft computing techniques. Moreover, they will be privy to the empirical evidence that highlights the strengths and weaknesses of each approach. Ultimately, this comprehensive analysis will serve as a valuable resource for researchers, practitioners, and decision-makers involved in hydrology and water resource management, guiding them towards informed choices when selecting modeling methodologies for their specific applications.